Materials Characterization 219 (2025) 114621

Contents lists available at ScienceDirect

Materials Characterization

journal homepage: www.elsevier.com/locate/matchar

HHF response of an optimized W-EUROFER joint brazed with pure copper

I. Izaguirre [a,*], D. Dorow-Gerspach [b], J. de Prado [a], M. Sánchez [a,c], M. Wirtz [b], A. Ureña [a,c]

[a] Materials Science and Engineering Area, ESCET, Rey Juan Carlos University, C/Tulipán s/n, 28933 Móstoles, Madrid, Spain
[b] Forschungszentrum Jülich GmbH, Institut für Energie- und Klimaforschung, 52425 Jülich, Germany
[c] Instituto de Investigación de Tecnologías para la Sostenibilidad, Universidad Rey Juan Carlos, C/ Tulipán s/n, 28933 Móstoles, Madrid, Spain

ARTICLE INFO

Keywords:
Tungsten
EUROFER
Brazing
Fusion reactor
High heat flux loads
Plasma facing component
Copper

ABSTRACT

The optimization of joint microstructure plays a critical role in assessing joint performance under high heat flux (HHF) conditions, as it dictates the final properties of the joint. This study investigates tungsten-EUROFER joints brazed using a copper interlayer as filler material under optimized brazing cycle conditions (1110 °C, 3 min), and subjected to simulated high heat fluxes exposing the plasma facing material, tungsten in this case, to a heating source (accelerated electron bean), while the joint is refrigerated through the EUROFER side. This experiment aims to mimic the heat fluxes and cooling conditions experienced in a fusion reactor environment. An optimized microstructure of the braze joint, designed to mitigate the formation of intermetallic compounds and undesirable phases, was implemented to enhance joint responses under high heat flux loads. The joints were subjected to 100 and 1000 heating-cooling cycles of 10/12 s. The target during heating is to reach the thermal equilibrium. Three different tungsten surface temperature were evaluated (600 °C, 700 °C and 800 °C) in different sample batches while cooling on the EUROFER side, removing the heat source during the cooling stage. Some overheating events, associated with crack propagation through the EUROFER-braze interface identified during the subsequent postmortem analysis by SEM, were detected during the application of some conditions of the test. The microstructure examination also reported a modification of the failure mechanism of the joint comparing with the previous studies and literature. This modification is associated with the optimized microstructure resulting in improved response to high heat flux loads. Interestingly, the shear strength increased to an average of 95.0 MPa after HHF testing, compared to 40.2 MPa obtained in similar joints with different microstructures.

1. Introduction

In recent decades, there has been a significant increase in energy consumption, highlighting the urgent need to explore new energy sources to meet this growing demand. As a result, considerable research and investment are focused on harnessing fusion energy as a promising alternative. A notable engineering effort in this field is the development of the DEMOnstration fusion reactor, which can launch the first commercial fusion reactor [1–3]. This project covers a thorough investigation across various disciplines. Among them, materials technology emerges as crucial, particularly in facilitating resistance under the anticipated extreme conditions within the reactor. Tungsten stands out as a key material for this application, attributed to its inherent properties, including remarkable resistance to sputtering and thermal loads, thereby raising prolonged operational durability [4,5]. The development of certain components for such reactors necessitates the joining of tungsten to a structural material, such as EUROFER or CuCrZr copper alloys.

Copper, under fusion reactor conditions, is widely recognized to be highly vulnerable to helium embrittlement, a phenomenon demonstrated by Fabritsiev and Pokrovsky [6]. The embrittlement process is primarily attributed to the accumulation of helium at grain boundaries due to irradiation. Therefore, this study exclusively employs a thin layer of copper as a filler material to join tungsten to reduced activation ferritic/martensitic steel (EUROFER) using the brazing technique. With this reduced thickness we aim to reduce this phenomenon, as only a few microns of interlayer remain after the process. Copper, serving as the filler material, plays a critical role in alleviating residual stresses that arise during the cooling phase of the thermal process. It is caused by the mismatch in the coefficient of thermal expansion (CTE) between the materials involved [7] and via plastic deformation of the Cu layer in between, this stress can be mitigated.

The use of copper as filler material has been explored by several authors, such as S. Zhao et al. [8], who optimized the brazing process to

* Corresponding author.
E-mail address: ignacio.izaguirre@urjc.es (I. Izaguirre).

https://doi.org/10.1016/j.matchar.2024.114621
Received 16 September 2024; Received in revised form 18 November 2024; Accepted 3 December 2024
Available online 5 December 2024

control the spreading parameters of the copper filler. They utilized copper alloys like CuGeNi and CuMnNi fillers to join tungsten to reduced activation ferritic/martensitic steel. Their research demonstrated that reducing the thickness of the filler and adjusting the brazing temperature effectively mitigated the loss of braze material, resulting in an ultimate tensile strength of up to 180 MPa. Additionally, addressing the significant difference in CTEs between tungsten and steel, D. Bachurina et al. [9] utilized a vanadium layer, complemented by a copper-based filler between these layers. The resulting steel/Cu-28Ti/V/Cu-50Ti/W and steel/Cu-50Ti/V/Cu-50Ti/W brazed joints underwent a series of heat treatments, each step impacting the microstructures and shear strength of the joints.

Before implementing the joint in the reactor, it is necessary to characterize not only the joint microstructure but also its performance under similar working conditions. To achieve this, High Heat Flux (HHF) tests can be employed to replicate the heat load and gradient an actively cooled plasma-facing component will have to endure inside a reactor. This technique has been utilized by several researchers, such as N. Nemati et al. [10], who investigated the recrystallization of tungsten during HHF tests and compared the microstructure of two different samples. One of these samples was subjected to well-defined furnace heat treatment conditions (1500 °C, 2100 °C), while the other was extracted from the monoblocks of a water-cooled mock-up and tested under HHF loads at 20 MW/m^2 for 500 cycles. The results revealed that the significant grain deformation likely contributed to the observed high Vickers hardness of the HHF sample, in contrast to steady-state heating at the same temperature. In a related study, D. Dorow-Gerspach et al. [11] explored various approaches to address the coefficient of CTE mismatch between tungsten and steel. While functionally graded material layers succeeded in reducing the CTE difference as anticipated, the components failed under higher heat fluxes, indicating that none of the joints prepared using this technique could withstand the same heat fluxes as those prepared via direct joining configuration.

This study builds upon prior efforts by focusing on the development and optimization of W-EUROFER joints for their application in the DEMO reactor [12–14]. Previous HHF tests utilizing the same filler material and brazed at 1135 °C demonstrated a favorable response up to temperatures of 700–800 °C [15]. However, mechanical characterization of the joints post-testing revealed a significant drop in mechanical properties, decreasing from 300 MPa in the as-brazed conditions to an average of 50 MPa after HHF testing. Postmortem analysis revealed fracture propagation along phases rich in Fe and Fe—W, located at the W-braze interface. Additionally, nearly all of the copper filler material exuded from the joint clearance during the brazing process, leaving only a copper layer of a few microns at the braze area.

Taking these results into account, a modification of the braze microstructure was considered, optimizing both brazing temperature and dwell time while analyzing in detail the formation and development of the microstructure. The results, as detailed in [15], aim to enhance the mechanical and HHF response by promoting the formation of a copper layer at the braze area capable of relieving the stress generated by the mismatch in the coefficients of thermal expansion of the base materials. This is particularly relevant since HHF tests involve continuous heating and cooling cycles, during which stress accumulates. The optimization also aims to prevent the formation of phases rich in iron at the W-braze interface, which tend to form at temperatures close to 1115–1130 °C [14]. The formation of these compounds adversely affects the mechanical response and reduces the toughness of the joint, leading to premature failure during previous HHF experiments on these types of joints.

This study seeks to determine the impact of simulating the heat flows within a reactor environment on the properties of joints between tungsten and EUROFER, utilizing copper as filler material with an optimized microstructure. The tests were conducted under controlled conditions, including heat flux, number of cycles, and heating time, to achieve steady-state conditions [13,15].

2. Joint design and HHF tests

The brazing process utilized the following base materials: i) Tungsten plates (>99.97 % purity, sourced from *Plansee*) and ii) Reduced activation ferritic/martensitic steel - EUROFER plates, characterized by a chemical composition in weight percentages of 0.11 % carbon (C), 8.9 % chromium (Cr), 0.42 % manganese (Mn), 0.19 % vanadium (V), 1.10 % tungsten (W), 0.14 % tantalum (Ta), with the remainder being iron (Fe) and with the following heat treatments 979 °C/1 h 51 min /air cooled plus 739 °C/3 h 42 min /air cooled [16,17].

Both base materials were provided in block form, each with an exposed surface area measuring 5 × 5 mm^2 and a thickness of 5 mm. The blocks were machined from the plate by electrical discharge machining technique. Pure copper (>99.9 % purity), the filler for the brazing process, was procured in the form of a 50 μm thick strip from *Lucas Milhaupt*. This strip was meticulously cut to match the dimensions of the exposed surfaces of the base materials and positioned between them. Before the brazing tests, the exposed surfaces of both base materials underwent preparation, involving grinding with up to 4000 grit silicon carbide paper. The brazing experiments were executed within a high vacuum furnace to prevent oxidation, maintaining a residual pressure of 10^{-4} Pa throughout. During the brazing process any additional force was applied but the weight of the upper base material, which is EUROFER (8 g approximately). The brazing cycle involved a heating up to 1110 °C sustained for 3 min, followed by cooling to room temperature utilizing heating and cooling ramps of 5 °C/min, following previous works that optimized the W-EUROFER microstructure using this Cu filler material [14].

Following the brazing process, a post-brazing heat treatment (PBHT), also known as a tempering treatment, was applied at 760 °C for a duration of 90 min using for that purpose the same furnace in a high vacuum atmosphere [13]. The objective of this heat treatment was to return the tempered martensite properties of the EUROFER material, along with its initial hardness level, which had been quantified at 216 HV prior to the brazing operation [18].

For the HHF tests, the specimens were fixed onto an actively cooled copper cooling structure, as a heat sink, which was connected to a water pipe. Brazing was selected as the preferred joining technique to ensure optimal thermal conductivity and metallic continuity between the specimens and the cooling structure, thereby facilitating efficient cooling during the experiments [19]. For this purpose, a tape-shaped filler material supplied by *STELLA WELDINGS ALLOYS* was utilized, composed of 56 % silver (Ag), 22 % copper (Cu), 17 % zinc (Zn), and 5 % tin (Sn) by weight. The joining process was conducted while incorporating the aforementioned tempering treatment to maintain the original microstructure of the materials without further alteration. The cooling structures and water pipes, along with the joints and the filler material employed for their attachment to the cooling structure, are depicted in Fig. 1a, while Fig. 1b presents a schematic diagram of the HHF tests.

The HHF tests were performed in the JUDITH 2 electron beam facility, located at the Forschungszentrum Jülich (FZJ). Cooling of the test specimens was accomplished through pressurized cooling water, supplied at an inlet pressure of 2 MPa and held at a constant temperature of 27 °C, with a nominal flow rate of 60 l/min. Throughout the experiments, continuous monitoring was conducted using an infrared (IR) camera and pyrometers to determine surface temperature, regulate the applied power density and detect any surface overheating due to inadequate cooling. It is noteworthy that the temperature readings obtained from the IR camera underwent cross-calibration with a two-color pyrometer. However, given the potential variation in emissivity properties among different samples, this calibration was specific to each individual sample, necessitating cautious interpretation of temperature data. Furthermore, the cross-calibration was performed at the beginning of each experiment, and any changes in emissivity during testing could lead to discrepancies between the readings obtained from the two-color pyrometer and those from the IR camera. The heating and cooling cycles

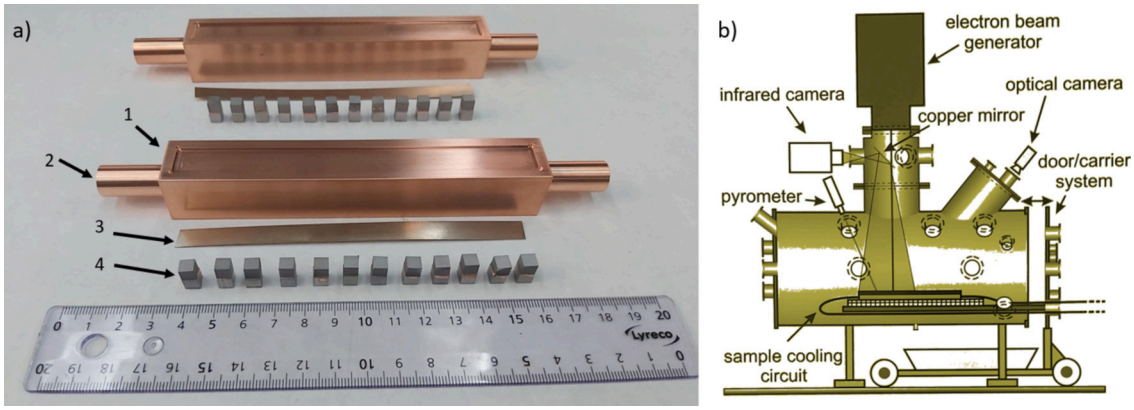

Fig. 1. (a) General view of cooling structure (numbered 1) with the brazed samples used for HHF tests (numbered 2), the water pipe (numbered 3) and the filler use to joint to cooling structure with the samples (numbered 4). (b) Schematic figure of machine Judith 2 which was used for the HHF test.

implemented in the HHF tests were designed to attain a state of thermal equilibrium, with heating and cooling durations of 10 s and 12 s, respectively. Additionally, the vacuum conditions within the JUDITH 2 facility maintained an oxygen partial pressure of approximately $5{\cdot}10^{-3}$ Pa.

A total of 24 joints underwent testing, organized into five batches, with each batch consisting of four samples. Within each batch, one sample was allocated for microstructural analysis and hardness testing, while the remaining three samples were designated for mechanical property assessment via shear tests. Each batch was subjected to distinct experimental conditions, specifically varying the tungsten surface temperature to 600 °C, 700 °C and 800 °C, and exposing them to different numbers of applied cycles, either 100 or 1000 cycles. Each surface temperature corresponded to specific power densities on the surface (T_{surf}) of approximately 1.5, 1.7, and 2 MW/m^2, respectively. Detailed experimental conditions for all tests are provided in Table 1.

Following the completion of HHF testing, the W-EUROFER joints were separated from the copper cooling structure using a diamond wire cutting technique. Microstructural analysis was conducted on these samples, which were prepared using a standard polishing technique, continuing until reaching a particle size of 1 um diamond, which is enough to resolve the phases and information relevant in this work. Subsequently, the prepared metallographic samples were subjected to microstructural examination by scanning electron microscopy (SEM, *S3400 Hitachi* model), equipped with an Energy Dispersive Spectroscopy (EDS) detector and the associated software. Additionally, a *Leica DFC320* stereoscopic microscope was employed for examination in some cases.

The determination of shear strength values was conducted using a compression device engineered to ensure the precise alignment of the brazed joint with the applied load. This design effectively eliminated any potential bending of the specimens during testing, thereby ensuring the application of pure shear stress on the brazed surface. Additional information regarding this test setup can be found in reference [20]. The testing fixture was positioned between the compression plates of a Universal Testing Machine (*Zwick Z100*) and operated at a controlled displacement rate of 1 mm/min. The standard deviation of the results will be calculated and plotted along with the main shear value to know the dispersion of the results.

To evaluate the potential impact of the brazing thermal cycle on the hardness characteristics of the base materials, Vickers microhardness testing was utilized. Microhardness profiles crossing from the EUROFER to the tungsten, through the brazed joint, were made using an *MHV-2 SHIMADZU* apparatus. A 100 g load was applied for 15 s, with three indentation tests conducted per profile from the center of the joint. It is noteworthy that the separation between adjacent indentations consistently exceeded three times the residual imprint sizes.

Table 1
Proposed HHF tests conditions for W-EUROFER joints.

Batch	W surface target temperature (°C)	Power density (MW/m^2)	Number of cycles
1	600	1.5	100
2	600	1.5	1000
3	700	1.7	100
4	700	1.7	1000
5	800	2	100

3. Results

3.1. HHF tests

Table 2 summarizes the results of the HHF tests, categorized by batch, and indicates the corresponding test conditions. The table provides additional information in cases where overheating i.e. sample

Table 2
Summary of HHF testing conditions and the phenomena occurred during the tests.

Batch	W surface target T / Bond surface T / Power density	Sample	Cycles applied	Additional information
1	600 °C / 498 °C / 1.5 MW/m^2	#1	100	–
		#2	100	–
		#3	100	Overheating in cycle 25
		#4	100	–
		#5	1000	–
2	600 °C / 498 °C / 1.5 MW/m^2	#6	1000	Overheating in cycle 250
		#7	1000	Overheating in cycle 300
		#8	1000	–
3	700 °C / 578 °C / 1.7 MW/m^2	#9	100	–
		#10	100	–
		#11	100	Overheating in cycle 33
		#12	100	–
		#13	160	–
4	700 °C / 578 °C / 1.7 MW/m^2	#14	160	Overheating in cycle 100
		#15	160	Overheating in cycle 100
		#16	160	–
5	800 °C / 656 °C / 2 MW/m^2	#17	100	–
		#18	100	–
		#19	100	Overheating in cycle 50
		#20	100	–

degradation occurred. In those cases, if the surface temperature exceeded 1000 °C, the tests were stopped in order to be well below the melting temperature of the Cu-filler. The overheated samples were analyzed by SEM to identify the cause of failure. The remaining samples were reserved for the mechanical characterization of the joint. Bond surface temperature data was obtained from previous works, where samples with the non-optimized microstructure was used for the HHF tests. The system, in both cases, uses similar temperatures, materials and dimensions so the results could be extrapolated to this experiment. ANSYS software was used for the FEM simulation [15].

Following the application of a 600 °C surface temperature, an increment to 700 °C - 1.7 MW/m^2 was implemented. During the application of this condition for 100 cycles, corresponding to batch number 3, only sample #11 exhibited overheating, detected at the end of the test. In this case, pyrometer readings exceeding 1000 °C. However, the remaining samples exhibited no degradation. Regarding batch number 4, chosen for 1000 cycles, testing was stopped after 160 cycles due to sample #15 overheating well beyond 1000 °C (Fig. 2c-d).

Finally, batch number 5 was subjected to 800 °C – 2 MW/m^2 on the tungsten surface. The application of these conditions resulted in overheating in sample #19 after 50 cycles. The recorded surface temperature exhibited a progressive increase, as depicted in Fig. 2b, provoking the termination of the test upon reaching a pyrometer reading of 1000 °C.

3.2. Microstructural analysis

Fig. 3a depicts the microstructure of the W-EUROFER joint within the brazed region following exposure to 100 cycles at 600 °C-1.5 MW/m^2. In this instance, the microstructure remains unaltered despite the application of heat flow, aligning closely with the optimized microstructure previously identified by the authors in their prior research works [14]. It comprises a copper layer approximately 40–50 μm thick, where the braze has initiated penetration, following grain boundary paths into the EUROFER base material, as illustrated by the white arrow in Fig. 3a. At the interface of copper and tungsten, a diffusion layer (labeled as number 1 in Fig. 3b) with a composition in at. % of 39W51Fe9Cr rich in Fe—W is observed. Additionally, above this phase, the presence of an iron-rich phase (labeled as number 2 in Fig. 3b) has been identified (EDS at. % 79Fe7W8Cr5Cu). This latter phase appears in minor areas of the interface, forming isolated islands.

However, when subjected to 1000 cycles under these conditions, crack formation at the interface between the braze and EUROFER is observed, even extending into the center of the joint, as indicated by the white arrow in Fig. 4a. The increased stress accumulation resulting from the higher number of cycles applied is responsible for the propagation of the crack from the edge towards the center, as illustrated in Fig. 4b and a, respectively. Thermal fatigue, which causes continuous expansion and shrinkage of the samples dimension and the temperature gradient in the different materials that conform the mock up also contribute to this phenomenon, due to the mismatch in the CTE of both base materials, as demonstrate in other works, where the residual stress generated during the HHF tests and brazing process were simulated by FEM [21,22]. Thermal simulations of HHF tests conducted in prior studies under the same surface temperature conditions indicate that the joint interface reaches 498 °C under these test conditions [15].

The increase in heat flux up to 700 °C-1.7 MW/m^2 resulted in overheating occurring at cycle 33 and 100 for batches 3 and 4, respectively. In the case of batch 3, all cycles (100) were completed as the temperature did not exceed the predetermined threshold. However, for batch 4, testing was stopped after 160 cycles due to the detection of temperatures reaching 1000 °C at the tungsten surface. The analysis of the sample microstructures from both failed samples after testing revealed discontinuities at the sample edges (Fig. 5b and Fig. 5d for 100 and 160 cycles, respectively), which were responsible for the observed thermal events. However, the propagation of the cracks did not extend to the center of the joint area (Fig. 5a and Fig. 5c, respectively).

Ultimately, subjecting the tungsten surface to 800 °C-2 MW/m^2 led to overheating of sample #19 after 50 cycles. Nevertheless, the temperature remained below 1000 °C, allowing the test to be completed as per the designated procedure. Fig. 6a and b display micrographs of the joint area post-test, revealing the presence of cracks at the sample edge that have the potential to hinder the heat flux.

Although, the microstructural observations have been conducted in the failed samples, remaining the others for mechanical characterization, the microstructural comparison between samples before and after the HHF tests, studied in reference [14], could inform about the nature of the overheating event. Samples in as brazed conditions did not report crack formation neither in the sample edge nor in the center. Therefore, those observations agree with the hypothesis that the crack formation during the HHF tests is the responsible of the overheating events.

3.3. Mechanical properties

In order to assess the impact of thermal fatigue on the mechanical properties of the joint following the tests, shear strength tests and Vickers microhardness analyses were conducted.

The results of the shear strength test, both after the HHF tests and under the initial braze conditions, are presented in Fig. 7. Subjecting the tungsten surface to 600 °C-1.5 MW/m^2 for 100 cycles a shear value of 98.5 ± 26.6 MPa is obtained. This value exceeds that of samples

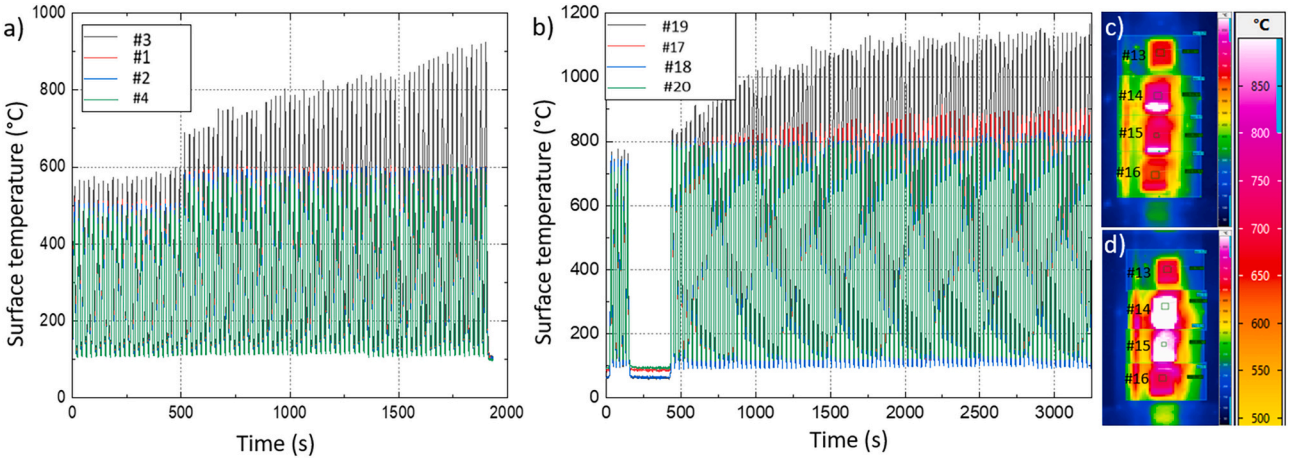

Fig. 2. Surface temperature record of the heating and cooling cycles for batches subjected to (a) 600 °C - 100 cycles and (b) 800 °C - 100 cycles. Comparison of IR images showing the overheating of the sample #15 subjected to 700 °C at (c) 1 cycle and (d) 160 cycles.

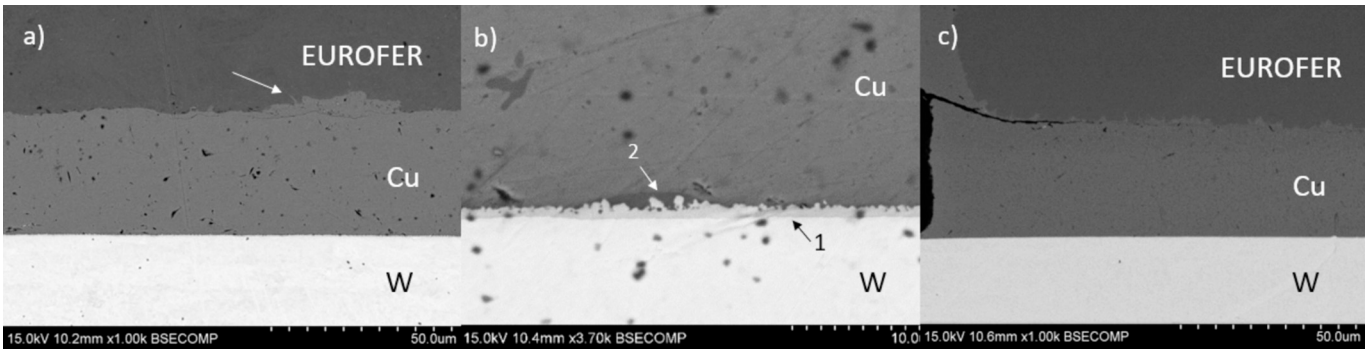

Fig. 3. SEM images sample #3 (600 °C-1.5 MW/m2 (a) General overview of the braze area. (b) Detail of the microstructure at the W-braze interface and (c) image corresponding with the sample edge, where crack formation appears.

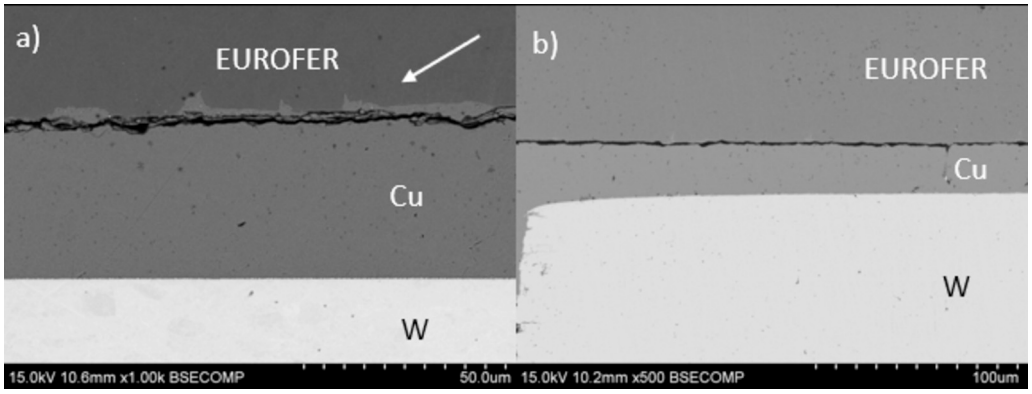

Fig. 4. Micrographs of sample #7 subjected to a W surface temperature of 600 °C for 1000 cycles: (a) center and (b) edge of the joint.

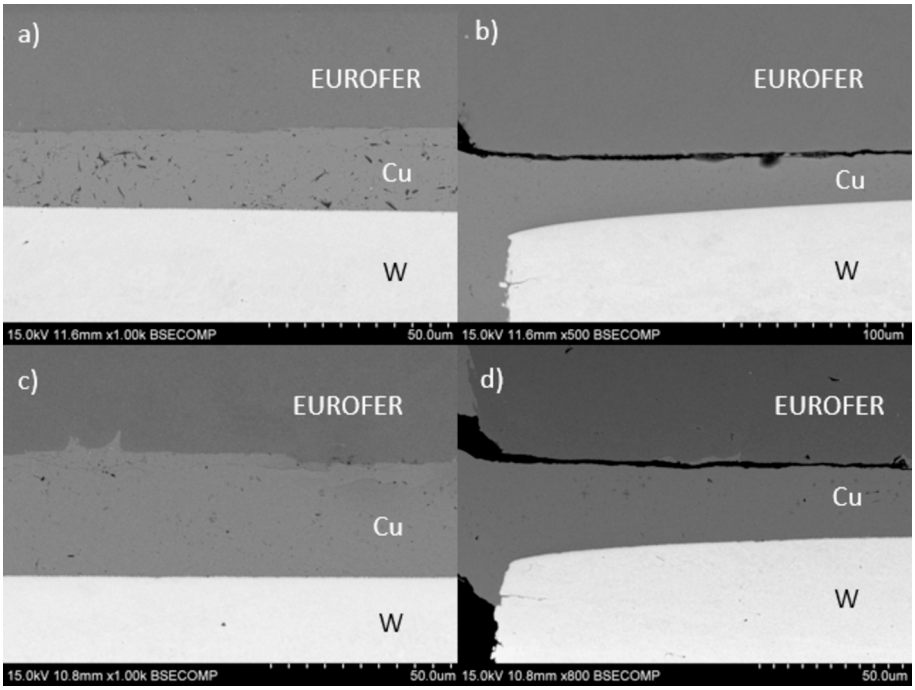

Fig. 5. Micrographs of sample #11 subjected to a W surface temperature of 700 °C for 100 cycles: (a) center and (b) edge of the joint. Micrographs of sample #14 after 160 cycles: (c) center and (d) edge of the joint.

subjected to 1000 cycles under the same surface temperature condition, which exhibited shear values of 67.4 ± 8.8 MPa. This observation aligns with HHF experimental results, indicating that an increase in applied cycles results in higher residual stress within the joint and the propagation of cracks from the edge towards the center, consequently leading to reduced strength. A similar trend is observed when applying 700 °C-

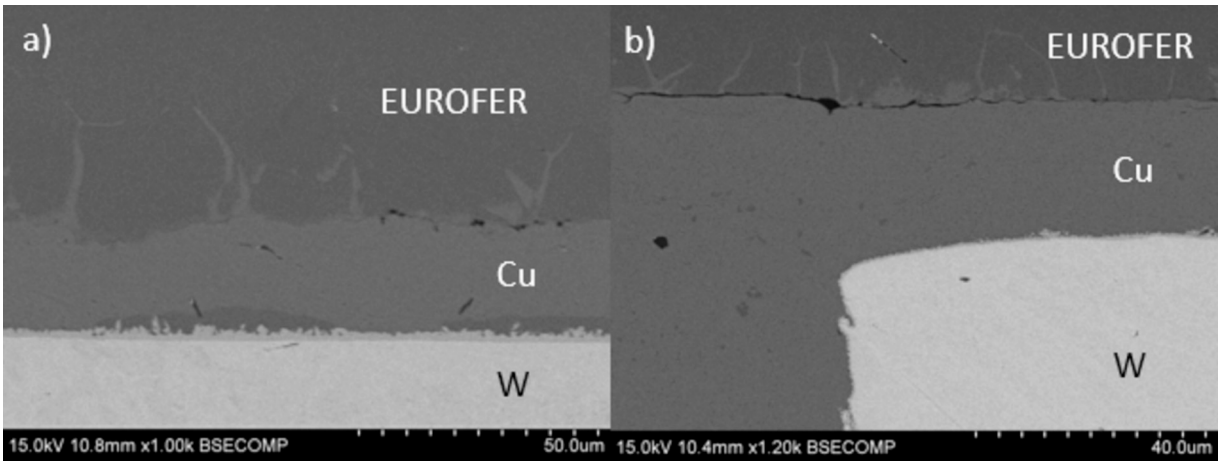

Fig. 6. Micrographs of sample #19samples subjected to a W surface temperature of 800 °C for 100 cycles: (a) center and (b) edge of the joint.

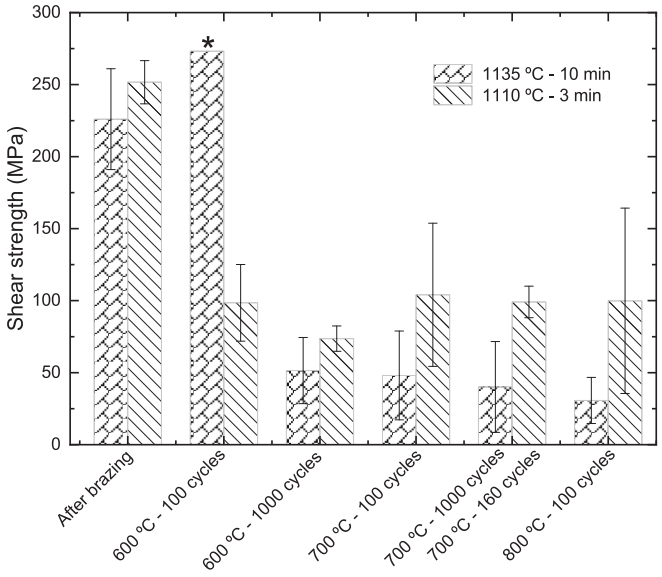

Fig. 7. Shear strength of W-EUROFER joints subjected to different HHF conditions of W surface temperature and number of cycles with the optimized (1110 °C – 3 min) and non-optimized microstructure (1135 °C – 10 min data taken from [15]). *In this case only one sample has been measured.

1.7 MW/m^2 to the tungsten surface, although in this instance, only 160 cycles could be completed in batch 4 and the mean values are within the error bar. Shear values after 100 cycles under this condition were reported as 102.1 ± 49.7 MPa, compared to 99.1 ± 11 MPa when 160 cycles were applied. Lastly, subjecting the surface to 800 °C-2 MW/m^2 resulted in shear values of 99.9 ± 48.3 MPa.

The comparison of these results against those of the non-optimized microstructure reveals an enhancement in the mechanical integrity of the samples post-testing, as illustrated in Fig. 7.

To complete the study, the fracture surface and cross-section cut of shear test was analyzed. All samples shown the same fracture mechanism characterized by the presence, in the center of the fracture surface, of a metallic color ring. Fracture surface of sample #12 subjected to 700 °C-1.7 MW/m^2 and 100 cycles was selected as representative fracture for its analysis in the present work (Fig. 8). It seems that the fracture, initiated by the crack propagation of the nucleated cracks during HHF tests, as the microstructural examination has determined, occurred at the sample edge along the EUROFER-braze interface (Fig. 8f and i). However, towards the center of the joint, the fracture propagation moved to the W-braze interface momentarily before reverting to the EUROFER-braze interface.

The analysis of the fracture surface is completed by a SEM examination. Fig. 9a shows W base material fracture surface, where the inner ring can be clearly observed showing a bright contrast. The elemental mapping distribution indicated the W nature of the ring and the remaining copper braze material in the rest of the surface. Those observation agrees with the fracture profile above described. Finally, the fracture surface shows a brittle fracture mode in both areas. Fig. 9b shows the EUROFER side of the fracture surface, where the tungsten detached from the base material could be observed in the inner ring. A mixture composition between Fe and Cu is observed on the rest of the sample, which indicated that the fracture path has followed the braze area where copper penetrates into the EUROFER base material.

The possible impact of the HHF tests in the base material hardness could reveal changes in the microstructure associated to the temperatures reached during the test. The results of the microhardness tests, applied as a hardness profile from one base material to the other, are shown in Fig. 10. It shows hardness values of approximately 450 $HV_{0.1}$ and 220 $HV_{0.1}$ for tungsten and EUROFER, respectively, similar to as-received conditions (216 ± 20 $HV_{0.1}$ and 450 ± 12 $HV_{0.1}$ for EUROFER and tungsten, respectively [14].

4. Discussion

4.1. HHF tests

The overheating events indicated the loss of refrigeration capabilities, possibly related to degradation at the W-EUROFER interface. Therefore, the heat transfer to the coolant was hindered due to the loss of metallic continuity, leading to surface overheating. Further overheating could approach the brazing temperature and could produce the melting of the braze, complicating the subsequent determination of the failure mechanism. This was only the case during testing batch 4, where 1000 cycles had been planned.

The test began by applying the 600 °C - 1.5 MW/m^2 condition to the tungsten surface. After 25 cycles, sample #3 exhibited degradation in its cooling capabilities, as indicated by an increase in measured temperature by the pyrometer to values exceeding 800 °C (Fig. 2a). However, the remaining samples demonstrated thermal stability. Consequently, it was decided to proceed with the tests, and the proposed 100 cycles were successfully applied to the other samples without encountering any further anomalies, as these samples maintained surface temperature values around the expected 600 °C for the extent of the test. In the case of batch 2, intended for 1000 cycles, samples #6 and #7 experienced overheating after 250 cycles, reaching a surface temperature of 900 °C.

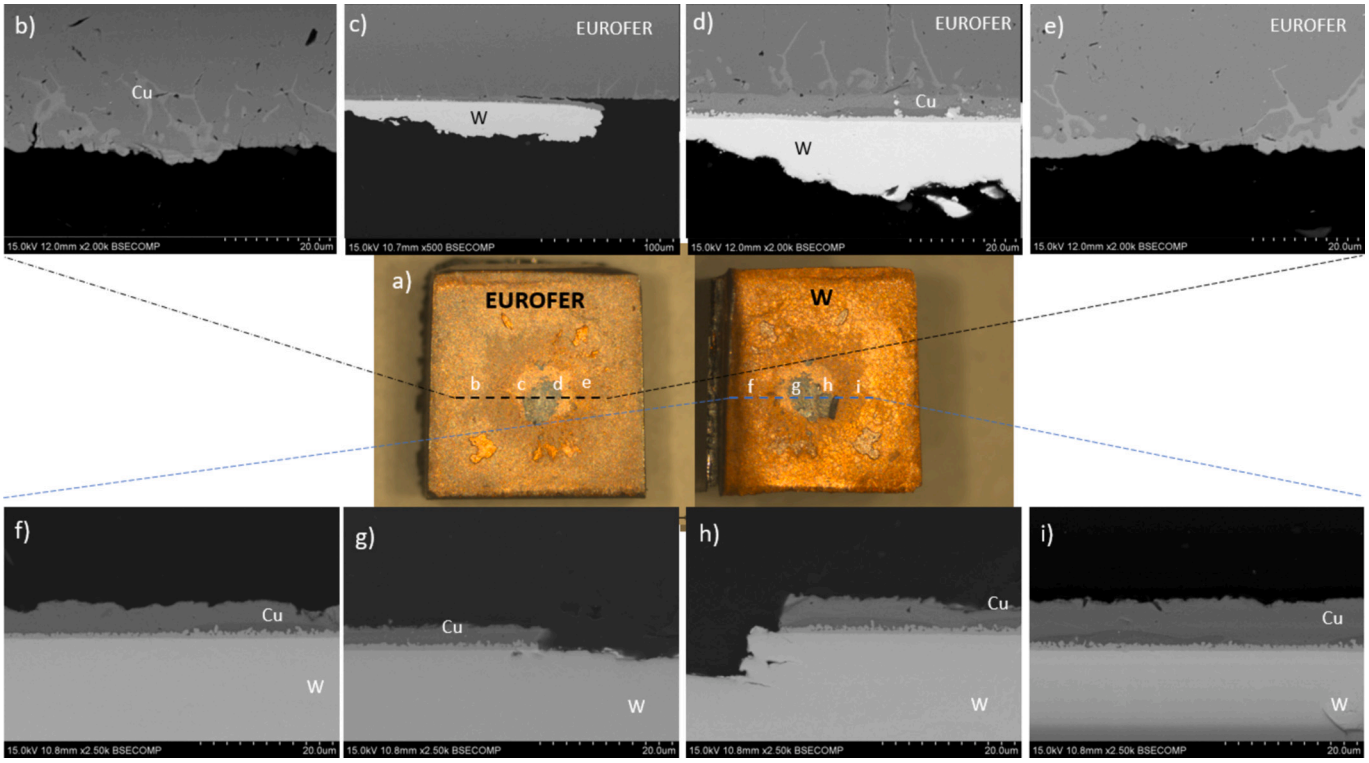

Fig. 8. (a) Stereoscopic image of fracture surfaces of sample #12 subjeted to 700 °C and 100 cycles after the shear test. Cross section images obtained by SEM following the dashed lines at (b), (c), (d) and (e) on EUROFER base material; and (f), (g), (h) and (i) on tungsten base material.

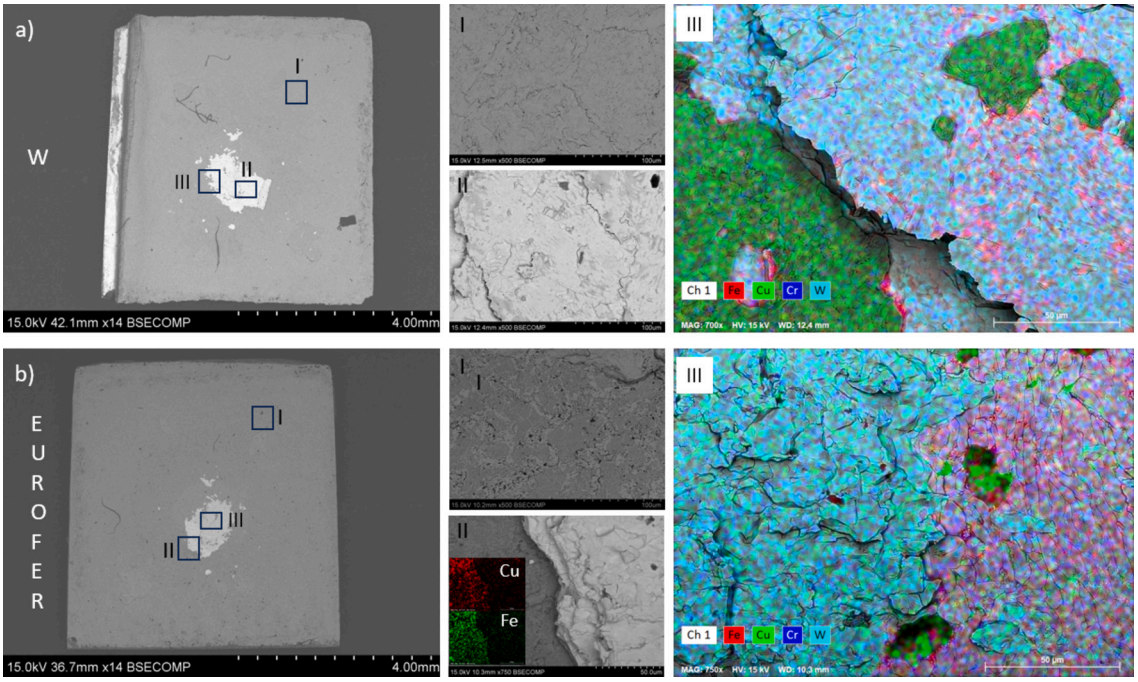

Fig. 9. SEM micrographs of fracture surface (a) W and (b) EUROFER with details and elemental distribution of details III in both surfaces.

However, the remaining samples in the batch exhibited no anomalies, maintaining the temperature throughout the entire 1000 cycles.

4.2. Microstructural analysis

The application of 100 cycles under these HHF conditions did not induce any alteration in the microstructure within the central region of the joint, according to microstructure in as brazed + PBHT conditions describe previous works, reference [14]. The metallic continuity at both interfaces, necessary for facilitating the transmission of heat flux from the heat source to the cooling medium, remains intact. However, the presence of cracks along the sample edge has been noted, as depicted in Fig. 3c. The formation of these cracks, aligned perpendicular to the heat flux, could potentially hinder heat transmission depending on their

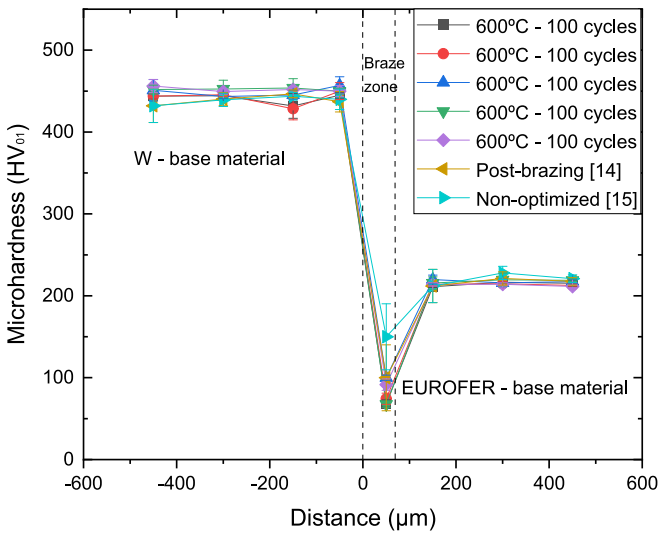

Fig. 10. Vickers microhardness profiles of W-EUROFER joints for the different HHF test conditions.

length and penetration into the joint area. In such cases, tungsten may not be effectively cooled by the coolant, resulting in the observed overheating phenomenon. The formation of these cracks can be attributed to the cumulative stress effect generated by each cycle of the test, due to the mismatch in coefficients of thermal expansion.

Previous studies examining HHF tests on W-EUROFER joints have revealed that stress accumulates with each cycle, typically at the edges of the joint [21,22]. These discontinuities tend to form and propagate along brittle phases at the W interface, as indicated by simulations conducted by other researchers assessing residual stress accumulation during thermal cycling [22]. This explanation is consistent with earlier investigations utilizing copper as a filler material with non-optimized microstructures, where cracks primarily formed between the iron-rich phase and the braze, near the W-braze interface. In such cases, the iron-rich phase formed a continuous layer approximately 5 μm thick at the interface [15], contrasting with the isolated islands observed in this study. Furthermore, the modification of the joints microstructure serves to prevent or control the formation of brittle phases at this interface, such as the diffusion layer, and, consequently, prevent the generation and propagation of cracks. Thus, the alteration of the microstructure has led to modifications in the mechanisms governing the crack formation and the propagation during the test.

Under 700 °C-1.7 MW/m^2 conditions the joint interface is subjected to 578 °C according to the thermal simulations [15]. This finding suggests that the upper region of the EUROFER side is exposed to temperatures exceeding those that typically induce softening of EUROFER, which is generally observed around 550 °C [23]. This demonstrated that this HHF tests place the joint in a simulated hard scenario of the reactor environment and the real operation should work with more conservative conditions.

Ultimately, subjecting the tungsten surface to 800 °C-2 MW/m^2, the propagation of these cracks appears to stop near the edge, possibly preventing excessive overheating and allowing the test to be concluded, despite the elevated surface temperature. Ideally, under these conditions (assuming perfect bond), the interface reached 656 °C, potentially altering the mechanical properties of the EUROFER base material due to its exposure to high temperatures.

4.3. Mechanical properties

It is evident from the Fig. 7 that the application of HHF tests results in a significant decrease in joint strength. This drop can be attributed to the continual accumulation of stress during each cycle. The relatively low CTE of tungsten, compared to other metals, leads to a substantial mismatch between the two base materials. The accumulation of stress and the consequent formation of discontinuities, particularly at the sample edge, are responsible for the observed reduction in joint strength [24,25].

It is important to highlight that, by using this optimized microstructure, there is not a clear trend between the increase of tungsten surface temperature or heat flux and the corresponding shear values reported. Apart from sample #7, none of the other samples utilized for mechanical characterization experienced any thermal events, and all completed the tests without any indication of degradation. Consequently, it appears that the mechanical integrity of the joints remained intact, with all samples yielding similar shear values. It is necessary to underline that the application of higher cycle numbers the influence could get substantial and must be verified in future experiments.

While an average shear strength of 50 MPa is achieved with the non-optimized microstructure, opting for the proposed microstructure yields an increase up to an average of 100 MPa. Only the sample subjected to 600 °C-100 cycles reported higher shear values using the non-optimized microstructure; however, it is important to consider that only one sample was tested in this case [15]. The observed increase in shear strength can be attributed to the modification of the fracture mechanism explained in the microstructural analysis section. With the microstructure optimization, cracks are prevented from nucleating at the W-braze interface, where the accumulation of residual stress typically promotes such occurrences. The absence of Fe-rich phase in the interface between copper and W following the microstructural optimization [14] inhibits crack nucleation and moves it to the EUROFER-braze interface. Therefore, degradation is more challenging, resulting in reduced mechanical degradation under similar applied conditions.

The alteration in the fracture mechanism resulted in the formation of a ring-shaped geometry evidenced in the fracture surface depicted in Fig. 8a. That's the typical fracture mechanism how joints fail/overheat subjected to conditions similar to that applied in this work [22,26–28]. From the edges the cracks are propagating towards the center till the occurring stress stays below the UTS, as stated before. The shear stress tests are performed at room temperature; thus W is brittle, and this causes the crack to be deflected a bit into the W-region. The thickness of the copper layer decreases slightly from the center to the edges of the joint due to exudation during the brazing process. The average thickness value of the braze in the center of the joint is 25 ± 6 μm, whereas at the edges of the samples this value increases up to 40 ± 4 μm. In principle, thicker copper braze would better mitigate the stress generated during the text, however thinner braze increase the brazeability, therefore optimum braze thickness is a challenging parameter that could be examined in other works. As a result, the fracture modifies the propagation mechanisms. The propagation does not strictly follow the W-braze interface but penetrates into the W base material, as shown in Fig. 8g and h and Fig. 9. In this case, tungsten remains adhered to the braze on the other side of the fracture, as depicted in Fig. 9c and d. This fracture mechanism indicates the high adhesion of the W-braze interface and the effect of the optimized microstructure, which inhibits the formation of continuous brittle phases, thereby modifying the typical propagation mechanism observed in other works [14].

Fig. 9 confirms that the absence of brittle phases at the interface with W prevents the crack from propagating through that interface. In Fig. 9a, at the interface of the W base material, the presence of copper can be seen in the entire interface, only W appearing in the middle of the sample, as shown in Fig. 8. However, the EUROFER interface shows the opposite side of the microstructure since the presence of iron associated with copper appears in the elemental analyses due to the penetration of the latter through the austenitic grain boundary of the steel during the brazing process.

The hardness values shown in Fig. 10 correspond to that obtained after the brazing process, therefore, the HHF test has not modified the hardness of the base materials [14]. Also, any difference with respect to

the non-optimized conditions was observed [15]. In the case of W, it remains constant at values close to 450 $HV_{0.1}$, which correspond to the hardness value of hot rolled polycrystalline tungsten [29]. In the case of EUROFER, values around 220 $HV_{0.1}$ correspond to the evolution of the microstructure carried out during the brazing and the PBHT thermal processes. The first process achieve the transformation of the austenite into martensite, after the austenitization that takes place above 890 °C during the brazing process, and the second one transform the martensite into tempered martensite typical of this steel [23].

5. Conclusions

The modification of the braze microstructure in W-EUROFER brazed joints, using copper as filler material and optimizing the brazing cycle with respect to previous studies (1110 °C - 3 min), has modified the crack propagation mechanism experimented by the joints during their exposure to high heat flux loads at 600 °C-1.5 MW/m2, 700 °C-1.7 MW/m2 and 800 °C-2 MW/m2 on the tungsten surface for 100 and 1000 cycles. The crack propagation, in the present work, follows the EUROFER-braze interface instead of the W-braze one, in which the stress is accumulated due to the mismatch in the CTE of both base materials. This modification is associated to the control of the braze microstructure obtaining a continuous copper braze of approximately 30 μm thick, in contrast to the non-optimized microstructure where discontinuous and thinner braze was formed. In addition, the suppression of intermetallic compounds and brittle phases was also achieved, which also contributed to the improved HHF respond.

Only one sample per condition showed overheating events during the tests and, with the exception of 700 °C-1000 cycles, all conditions could be applied. The shear strength of the joints after the tests halved compared to the one after brazing. However, it is roughly doubled compared to the 50 MPa obtained for the non-optimized joint tested previously [15]. The microhardness characterization showed that none of the base materials hardness was affected by the tests remaining the hardness as under as-brazed conditions.

CRediT authorship contribution statement

I. Izaguirre: Writing – original draft, Visualization, Validation, Methodology, Investigation, Formal analysis, Data curation. **D. Dorow-Gerspach:** Writing – original draft, Visualization, Validation, Methodology, Investigation, Formal analysis, Data curation. **J. de Prado:** Writing – original draft, Visualization, Validation, Methodology, Investigation, Formal analysis, Data curation. **M. Sánchez:** Writing – review & editing, Visualization, Supervision, Resources, Project administration, Investigation, Funding acquisition, Formal analysis, Conceptualization. **M. Wirtz:** Writing – review & editing, Visualization, Supervision, Resources, Project administration, Investigation, Funding acquisition, Formal analysis, Conceptualization. **A. Ureña:** Writing – review & editing, Visualization, Supervision, Resources, Project administration, Investigation, Funding acquisition, Formal analysis, Conceptualization.

Declaration of competing interest

The authors declare the following financial interests/personal relationships which may be considered as potential competing interests.

Ignacio Izaguirre reports financial support was provided by Rey Juan Carlos University.

Acknowledgments

This work has been carried out within the framework of the EUROfusion Consortium, funded by the European Union via the Euratom Research and Training Programme (Grant Agreement No 101052200 — EUROfusion). Views and opinions expressed are however those of the author(s) only and do not necessarily reflect those of the European Union or the European Commission. Neither the European Union nor the European Commission can be held responsible for them.

Data availability

Data will be made available on request.

References

[1] R. Kembleton, M. Siccinio, F. Maviglia, F. Militello, Benefits and challenges of advanced Divertor configurations in DEMO, Fusion Eng. Des. 179 (2022) 113120, https://doi.org/10.1016/j.fusengdes.2022.113120.
[2] Y. Someya, K. Tobita, R. Hiwatari, Y. Sakamoto, Fusion DEMO reactor design based on nuclear analysis, Fusion Eng. Des. 136 (2018) 1306–1312, https://doi.org/10.1016/j.fusengdes.2018.04.129.
[3] R. Kembleton, Technological features of a commercial fusion power plant, and the gap from DEMO, Fusion Eng. Des. 190 (2023) 113544, https://doi.org/10.1016/j.fusengdes.2023.113544.
[4] C. Luo, L. Xu, L. Zong, H. Shen, S. Wei, Research status of tungsten-based plasma-facing materials: a review, Fusion Eng. Des. 190 (2023) 113487, https://doi.org/10.1016/j.fusengdes.2023.113487.
[5] X. Wang, W. Qing Qin, F. Jiao, L. Yang Dong, J. Gen Guo, J. Zhang, C. Ren Yang, Review of tungsten resource reserves, tungsten concentrate production and tungsten beneficiation technology in China, Trans. Nonferrous Met. Soc. China (English Ed.) 32 (2022) 2318–2338, https://doi.org/10.1016/S1003-6326(22)65950-8.
[6] S.A. Fabritsiev, A.S. Pokrovsky, Neutron irradiation induced high temperature embrittlement of pure copper, Plasma Devi. Oper. 5 (1997) 133–141, https://doi.org/10.1080/10519999708228025.
[7] K. Li, J. Shan, C. Wang, Z. Tian, The role of copper in microstructures and mechanical properties of laser-welded Fe-19Ni-3Mo-1.5Ti maraging steel joint, Mater. Sci. Eng. A 681 (2017) 41–49, https://doi.org/10.1016/j.msea.2016.10.039.
[8] S. Zhao, Y. Zhang, T. Zhang, G. Song, M. Zhang, G. Luo, Fabrication of a W/cu/steel mock-up via optimizing the brazing parameters, Fusion Eng. Des. 195 (2023) 113941, https://doi.org/10.1016/j.fusengdes.2023.113941.
[9] D. Bachurina, A. Suchkov, J. Gurova, M. Savelyev, P. Dzhumaev, I. Kozlov, R. Svetogorov, M. Leont'eva-Smirnova, O. Sevryukov, Joining tungsten with steel for DEMO: simultaneous brazing by cu-Ti amorphous foils and heat treatment, Fusion Eng. Des. 162 (2021) 112099, https://doi.org/10.1016/j.fusengdes.2020.112099.
[10] N. Nemati, A. Manhard, H. Greuner, K. Hunger, B. Böswirth, E. Visca, J.H. You, Microstructural evolution of tungsten under thermal loads: a comparative study between cyclic high heat flux loading and isochronous furnace heating, Nucl. Mater. Energy 36 (2023) 101465, https://doi.org/10.1016/j.nme.2023.101465.
[11] D. Dorow-gerspach, M. Bram, V. Ganesh, J. Matejicek, G. Pintsuk, M. Vilemova, M. Wirtz, C. Linsmeier, Benchmarking by high heat flux testing of W-steel joining technologies, Nucl. Mater. Energy 37 (2023) 101508, https://doi.org/10.1016/j.nme.2023.101508.
[12] I. Izaguirre, M. Roldán, J. de Prado, V. Bonache, M. Sánchez, A. Ureña, S/TEM examination and nanomechanical response of W-Eurofer joints brazed with cu interlayers, Nucl. Mater. Energy 31 (2022) 101155, https://doi.org/10.1016/j.nme.2022.101155.
[13] J. de Prado, M. Sánchez, A. Ruiz, A. Ureña, Effect of brazing temperature, filler thickness and post brazing heat treatment on the microstructure and mechanical properties of W-Eurofer joints brazed with cu interlayers, J. Nucl. Mater. 533 (2020) 152117, https://doi.org/10.1016/j.jnucmat.2020.152117.
[14] I. Izaguirre, J. De Prado, M. Sánchez, A. Ureña, Wettability and microstructural evolution of copper filler in W and EUROFER brazed joints, 2024.
[15] I. Izaguirre, T. Loewenhoff, J. de Prado, M. Sánchez, M. Wirtz, V. Díaz-Mena, A. Ureña, Thermal fatigue response of W-EUROFER brazed joints by the application of high heat flux loads, J. Mater. Process. Technol. 319 (2023), https://doi.org/10.1016/j.jmatprotec.2023.118056.
[16] K. Mergia, N. Boukos, Structural, thermal, electrical and magnetic properties of Eurofer 97 steel, J. Nucl. Mater. 373 (2008) 1–8, https://doi.org/10.1016/j.jnucmat.2007.03.267.
[17] J. de Prado, M. Sánchez, M.V. Utrilla, M.D. López, A. Ureña, Study of a novel brazing process for W-W joints in fusion applications, Mater. Des. 112 (2016) 117–123, https://doi.org/10.1016/j.matdes.2016.09.067.
[18] P. Fernández, A.M. Lancha, J. Lapeña, M. Hernández-Mayoral, Metallurgical characterization of the reduced activation ferritic/martensitic steel Eurofer'97 on as-received condition, Fusion Eng. Des. 58–59 (2001) 787–792, https://doi.org/10.1016/S0920-3796(01)00563-4.
[19] Y. Li, C. Chen, R. Yi, Y. Ouyang, Review: special brazing and soldering, J. Manuf. Process. 60 (2020) 608–635, https://doi.org/10.1016/j.jmapro.2020.10.049.
[20] J. de Prado, M. Sánchez, A. Ureña, Evaluation of mechanically alloyed cu-based powders as filler alloy for brazing tungsten to a reduced activation ferritic-martensitic steel, J. Nucl. Mater. 490 (2017) 188–196, https://doi.org/10.1016/j.jnucmat.2017.04.033.
[21] T. Emmerich, D. Qu, R. Vaßen, J. Aktaa, Development of W-coating with functionally graded W/EUROFER-layers for protection of First-Wall materials, Fusion Eng. Des. 128 (2018) 58–67, https://doi.org/10.1016/j.fusengdes.2018.01.047.

[22] V. Díaz-Mena, J. de Prado, M. Roldán, I. Izaguirre, M. Sánchez, M. Rieth, A. Ureña, Numerical and experimental development of cupronickel filler brazed joints for divertor and first wall components in DEMO fusion reactor, J. Nucl. Mater. 588 (2024), https://doi.org/10.1016/j.jnucmat.2023.154830.
[23] Z. Lu, R.G. Faulkner, N. Riddle, F.D. Martino, K. Yang, Effect of heat treatment on microstructure and hardness of Eurofer 97, Eurofer ODS and T92 steels, J. Nucl. Mater. 386–388 (2009) 445–448, https://doi.org/10.1016/j.jnucmat.2008.12.152.
[24] J.H. You, H. Greuner, B. Böswirth, K. Hunger, S. Roccella, H. Roche, High-heat-flux performance limit of tungsten monoblock targets: impact on the armor materials and implications for power exhaust capacity, Nucl. Mater. Energy 33 (2022), https://doi.org/10.1016/j.nme.2022.101307.
[25] H.C. Kim, E. Bang, K.M. Kim, Y. Oh, H.N. Han, J. Choi, S.H. Hong, Analysis of hardness and microstructural changes in tungsten mono-blocks exposed to high heat flux at 10 MW/m2, Fusion Eng. Des. 170 (2021) 112530, https://doi.org/10.1016/j.fusengdes.2021.112530.
[26] J. de Prado, M. Sánchez, I. Izaguirre, D. Swan, A. Ureña, Exploring cu-Ge alloys as fillers materials for high vacuum brazing application of W and Cucrzr, SSRN Electron. J. (2022), https://doi.org/10.2139/ssrn.4025186.
[27] Y. Xu, X. Qiu, S. Wang, C. Wu, J. Su, F. Xing, Microstructures, mechanical properties and formation mechanisms of tungsten heavy alloy brazed joints using cu-Ti-Ni-Zr amorphous filler, Mater. Des. 223 (2022) 111181, https://doi.org/10.1016/j.matdes.2022.111181.
[28] V.O. Kirillova, N.S. Popov, J.A. Gurova, D.M. Bachurina, X. Tan, I.V. Fedotov, A. N. Suchkov, Brazing SMART tungsten alloys to RAFM steels by titanium-zirconium-beryllium brazing alloy, Fusion Eng. Des. 201 (2024) 114297, https://doi.org/10.1016/j.fusengdes.2024.114297.
[29] H.C. Kim, E. Bang, G. Min, H. Choi, H.N. Han, Analysis of high heat flux tested tungsten mono-blocks by hardness and microstructural profiling, Fusion Eng. Des. 193 (2023) 113800, https://doi.org/10.1016/j.fusengdes.2023.113800.